International Journal of Energy
ISSN: 2957-9473 | Vol. 5, No. 3, 2024

The Reservoir Characteristics Analysis of the G162 Area in the Jiyuan Oilfield, Yan 9 Segment.

Haoyu Ji

School of Earth Sciences and Engineering, Xi'an Shiyou University, Xi'an Shaanxi, 710065, China

Abstract: The G162 block of Jiyuan Oilfield in the Yan 9 segment has good exploration prospects, with multiple drilling wells yielding high industrial oil flow. However, current research on the reservoir characteristics of the Yan 9 segment in the G162 block is relatively weak, which has hindered the progress of exploration and development. To clarify the reservoir development characteristics of the Yan 9 segment in the G162 block of Jiyuan Oilfield, this study takes the reservoir of the Yan 9 segment in the G162 block of Jiyuan Oilfield as the research object, and conducts a study on the petrological characteristics, physical properties, and pore structure of the reservoir rocks by combining core samples, thin sections, physical properties, and high-pressure mercury injection data. The results show that the permeability and porosity of the Yan 9 segment reservoir vary greatly, with medium-sized pores and moderate permeability predominating, and the overall pore structure is relatively good. Based on the physical property data, types of pores, the curve shapes of high-pressure mercury injection, and various parameters, the pore structure of the Yan 9 segment reservoir is classified from good to poor into three types: I, II, and III. The study area is mainly dominated by Type II, followed by Type I.

Keywords: Jiyuan Oilfield; Yan 9 Segment; Reservoir Characteristics: Pore Structure.

1. Introduction

The Ordos Basin, as one of the most important oil and gas basins in central China, is extremely rich in oil and gas resources. By the end of 2022, in the Changqing exploration area of the Ordos Basin, the cumulative proven geological reserves of oil reached 68.3×10^8 tons, with an additional proven oil reserves exceeding 3×10^8 tons for 12 consecutive years; the cumulative proven reserves of natural gas reached 6.86×10^{12} m^3, with an additional proven geological reserves exceeding 2000×10^8 m^3 for 16 consecutive years; in 2022, the oil and gas production equivalent broke through 6.5×10^7 tons, providing strong support for national energy security. The Jiyuan Oilfield is an oil and gas-rich area within the Ordos Basin, with proven oil and gas reserves in the area and its surroundings reaching tens of millions of tons. The Yan 9 segment has always been the main exploration layer of the Jiyuan Oilfield G162 area in the early stage, but with the continuous deepening of exploration in the study area, a batch of high-yield oil wells have been drilled in the Yan 9 segment, indicating that the Yan 9 segment of the Jiyuan Oilfield G162 area has good exploration prospects. However, due to the small number of wells drilled through the Yan 9 segment in the early stage of the Jiyuan Oilfield G162 area, and the research has been mainly focused on sedimentary facies and sedimentary environment, the study on reservoir characteristics is weak, which has restricted the progress of oil and gas exploration and development in the area. Based on core physical property testing, thin sections, and mercury injection data, this paper conducts a study on the basic characteristics of rock types, reservoir space, pore structure, and reservoir physical properties of the Yan 9 segment in the Jiyuan Oilfield G162 block, in order to provide a reference for further oil and gas exploration in the Yan 9 segment of the Jiyuan Oilfield G162 area.

2. Geological Feature Analysis of the Yan 9 in the G162 Area of the Jiyuan Oilfield, Ordos Basin.

At the end of the Late Triassic, the Ordos Basin was affected by the Indosinian movement, which led to the uplift of the structure, causing the Triassic strata to be weathered and eroded. By the early Jurassic Fuxian period, the sedimentation was mainly characterized by filling and compensation. The study area focuses on the early Jurassic Yan'an Formation, which inherited the stratigraphic characteristics of the Fuxian Formation during the early Jurassic, primarily consisting of fluvial-lacustrine delta to riverine depositional systems. The Yan'an Formation has well-developed fluvial deltaic sedimentation, with a significant proportion of conglomerates and sandstones, making it an advantageous area for oil and gas accumulation. In addition, coal beds also developed in the depression swamp areas. The Yanshan movement caused the strata at the top of the Yan'an Formation in the study area to be missing, with the Zhiluo Formation directly overlying it. In the Jiyuan Oilfield G162 area, the main reservoir layer Yan 9 has a considerable sand body thickness, with an average combined thickness of 15.8m; the oil layer group of Yan 9 in the Jiyuan Oilfield G162 area has an oil layer thickness of about 11.3m, with some local oil layers being thicker; under strong hydrodynamic conditions, multiple river channels are superimposed, with the sand body in the middle of the river channel being thicker, exhibiting strong vertical and horizontal reservoir heterogeneity. The Yan 9 oil layer group in the study area is rich in vertical argillaceous interlayers, with thin single sand bodies and interbedded sand and mud on the flanks of the river channels, developing a mixture of fine sandstones, siltstones, mudstones, and coal, with single sand body thickness generally reaching 7m. The lateral continuity of the sand body in the Yan 9 section is poor, with a limited extension range, and the river channel sand bodies are often

separated by argillaceous interlayers. The three-dimensional seismic profiles and field outcrops show that the reservoir has rapid lithological changes in the horizontal direction, with a common phenomenon of sand body extinction, and the lateral continuity of sand body development is poor.

3. Reservoir Characteristics Analysis of the Yan 9 in the G162 Area of the Jiyuan Oilfield.

3.1. Reservoir Petrologic Characteristics

Through core observation and thin-section identification data statistics of the G162 area, the Yan 9 reservoir is primarily composed of coarse-medium grained feldspathic quartz sandstone. The reservoir in the study area is dominated by feldspathic sandstone, followed by lithic feldspathic sandstone; the clastic components account for 84.17%, and the interstitial materials account for 15.83%. Among the clastic particles, quartz content is 64.67%, feldspar 11.33%, and lithic fragments 8.17%. The interstitial materials are primarily composed of silty clay, kaolinite, siliceous material, and dolomite, at 1.89%, 1.73%, and 1.1% respectively (Figure 1). The main particle size range of the Yan 9 reservoir is 0.1~0.7mm, with a medium-grained structure being predominant; the particle sorting is moderate, and the clasts are mainly sub-angular to sub-rounded, with good rounding; the particles mainly make point contacts; the pore types are predominantly intergranular pores, followed by intergranular dissolution pores, lithic dissolution pores (biotite cleavage dissolution pores), feldspar grain internal dissolution pores, and cast mold pores, etc. The cementation types are mainly vuggy cementation, followed by matrix cementation, kaolinite cementation, etc., with quartz overgrowth being relatively rare. Therefore, the petrological characteristics of the Yan 9 reservoir mainly manifest as medium-low compositional maturity and medium-high textural maturity.

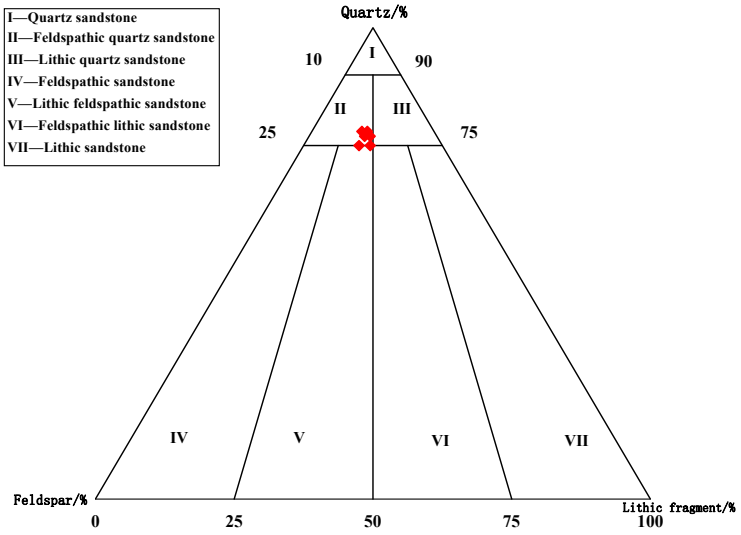

Figure 1. Triangular projection diagram of rock types in the G162 area of the Jiyuan Oilfield, Yanchang Formation, oil layer group

3.2. Reservoir Physical Properties

Based on the statistical analysis of conventional core physical property data from the G162 area (Figure 2), the porosity of the Yan 9 reservoir section ranges from 10% to 22%, with an average of 16%, primarily distributed between 18% and 20%, accounting for 50% of the total number of samples, and samples with porosity between 16% and 18% account for 29%; the permeability ranges from 0.1×10^{-3} to $1000\times10^{-3}\mu m^2$, with an average of $58\times10^{-3}\mu m^2$, mainly distributed between 10×10^{-3} and $100\times10^{-3}\mu m^2$, representing 55% of the total number of samples, and samples with permeability between 100×10^{-3} and $500\times10^{-3}\mu m^2$ account for 38%, classifying it as a medium-pore, medium-permeability reservoir. The porosity and permeability of the Yan 9 reservoir section exhibit a strong positive correlation (Figure 3). According to the core permeability test data, the Yan 9 reservoir section in the study area shows significant variations in pore size and permeability, with a predominance of medium-pore, medium-permeability characteristics, and an overall good pore structure.

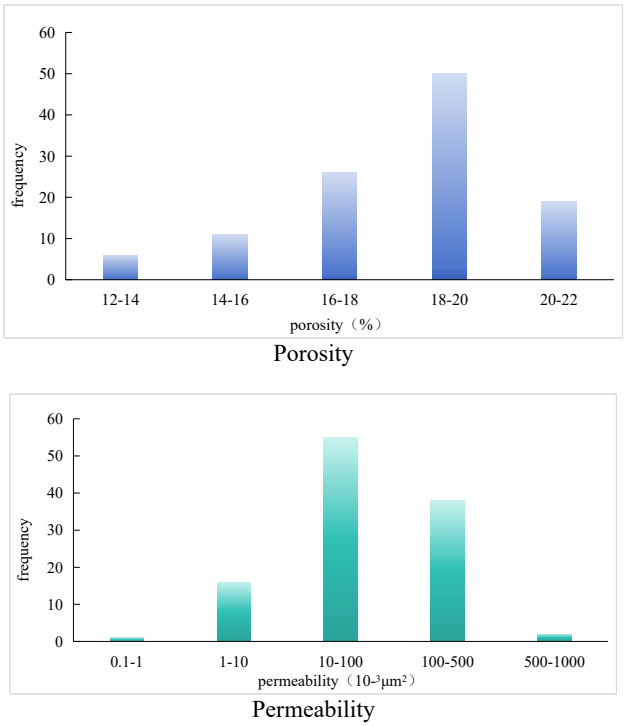

Figure 2. Frequency Distribution of Porosity and Permeability of Core Samples from the Yan 9 Section in the Study Area.

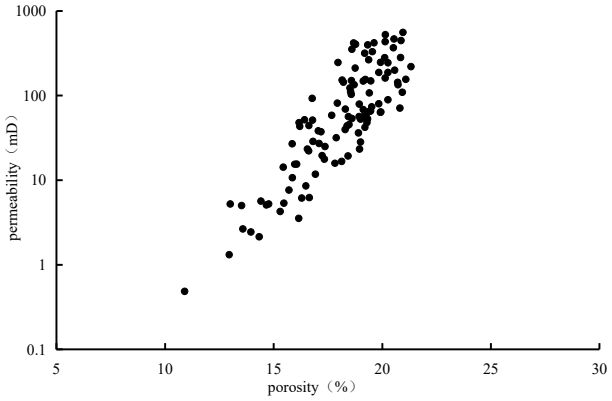

Figure 3. Cross-Plot of Porosity vs. Permeability for Core Samples from the Yan 9 Section in the Study Area

3.3. Pore Types in the Reservoir

Through the observation and analysis of the cast thin sections from the study area, it is known that the pores in the Yan 9 reservoir section of the G162 area are primarily residual intergranular pores, followed by intragranular dissolution pores (Figure 4). Intergranular pores are the most developed in the study area and are the main type of reservoir space. Under the microscope, they are mostly triangular or pentagonal, with a pore size ranging from 20 to 200μm, and some are filled with kaolinite, calcite, and quartz secondary overgrowth cement.

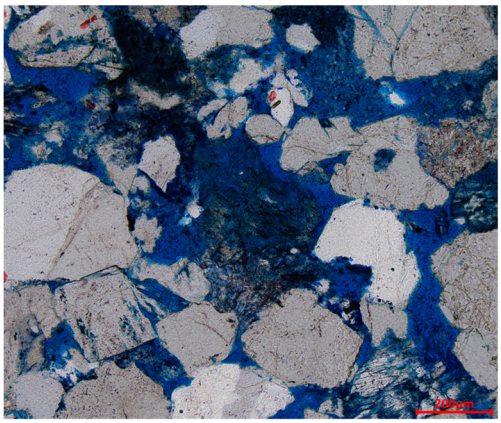

Intergranular pores

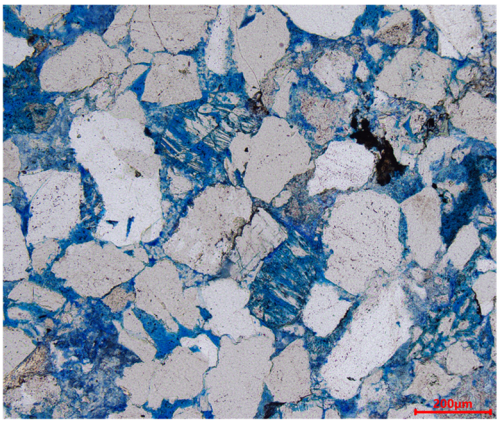

Intragranular dissolution pores

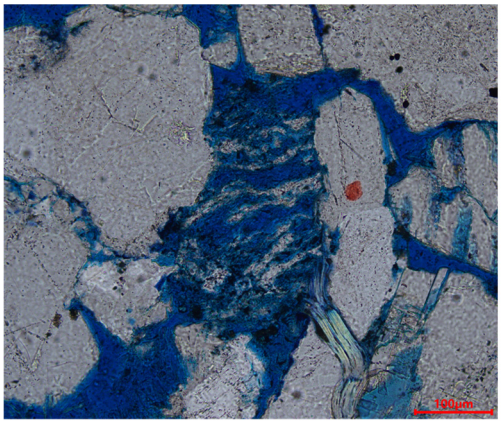

hydrocarbon residues observed within the edges of quartz overgrowths

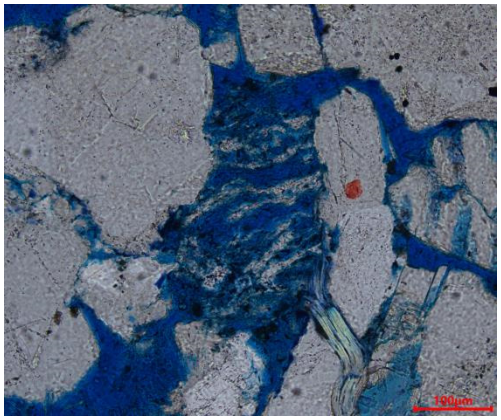

Feldspar casting pores

Figure 4. Pore Types in the Yan 9 Section of the Study Area

3.4. Pore Structure Characteristics in Reservoirs

By analyzing the mercury injection data from the core samples of the Yan 9 section within the study area (Table 1): the displacement pressure ranges from 0.027 to 0.096 MPa, with an average value of 0.054 MPa; the median pressure ranges from 0.22 to 1.40 MPa, with an average value of 0.72 MPa. The relatively low displacement and median pressures indicate that the sandstone in the study area has good sorting and reservoir pore structure, allowing for significant mercury intrusion at lower pressures, which suggests good permeability. The median throat radius ranges from 0.527 to 3.396 μm, with an average value of 2.315 μm, and the maximum pore throat radius ranges from 7.639 to 26.793 μm, with an average of 18.104 μm. In all samples, 78% of the samples have median throat radii and maximum throat radii greater than 4.76 and 19 μm, respectively, indicating that the

reservoir pore structure in the Yan 9 section of the study area is relatively good, with relatively coarse pore throats, dominated by medium-sized throats. The small volume of unsaturated mercury suggests that the reservoir in the study area has good connectivity and fewer micro-pore throats.

Table 1. Statistics of Mercury Injection Parameters for the Yan 9 Reservoir Section in the Study Area.

Parameter	Maximum Value	Minimum Value	Average Value
Porosity/%	21.32	10.9	18.1
Permeability/$10^{-3}\mu m^2$	0.48	559.4	113.8
Displacement pressure/MPa	0.096	0.027	0.054
pressure at 50% mercury saturation/MPa	1.40	0.22	0.72
median pore-throat radius/μm	3.396	0.527	2.315
Maximum throat radius. /μm	26.793	7.639	18.104
Mercury unsaturated volume/%	19.69	3.19	13.15
Mercury removal efficiency/%	32.46	9.12	17.75

Based on physical property data, types of porosity, the shape of high-pressure mercury injection curves, and various parameters, the pore structure of the Lower Member 4 sands in the study area is classified from best to worst into three types: I, II, and III.

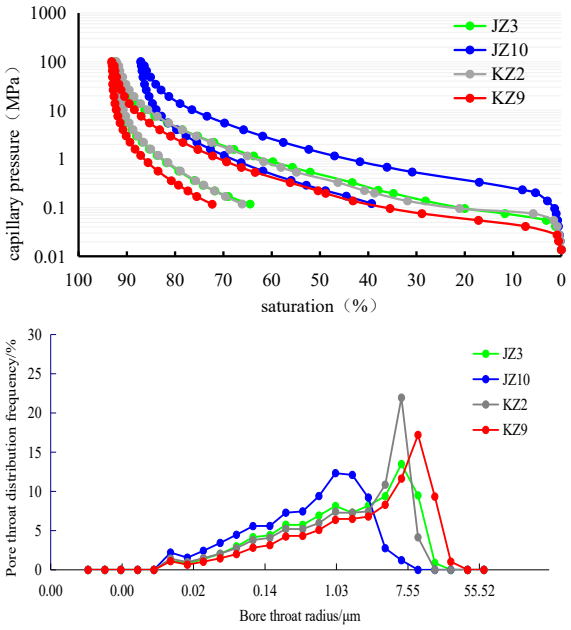

Figure 5. Mercury injection curve characteristics of the reservoir in the G162 area of the Jiyuan Oilfield, Yanchang Formation, Section 9.

Type I curve morphology exhibits a distinct coarse skewness characteristic, with the curve overall leaning towards the lower left, a long frequency plateau, and good sorting of pore throats; the proportion of pore throats greater than 10μm is the largest, often around 50%, and can reach more than 70% locally, with a low displacement pressure and median pressure, displacement pressure less than 0.03MPa, median pressure less than 0.3MPa, mercury unsaturated volume less than 15%, corresponding to the KZ9 sample. The pore structure of Type I corresponds to high-permeability high-porosity reservoirs, which are the best reservoir types in the study area, with porosity greater than 23% and permeability greater than $500\times10^{-3}\mu m^2$. The reservoir rocks corresponding to this pore structure are mainly medium to fine sandstones, with the main storage spaces being residual intergranular pores and a small amount of intragranular dissolution pores.

Type II pore structure has relatively finer pore throats compared to the Type I pore structure curve, with the overall curve slightly leaning towards the upper right, indicating poorer connectivity and reduced permeability of the reservoir; the pore throats are mainly concentrated between 7 to 10μm, accounting for more than 50%; the straight section of the curve is relatively short, reflecting a certain degree of sorting of the pore throats, but with poor sorting; its curve has a low to medium displacement pressure, with a displacement pressure of 0.03 to 0.05 MPa, a medium to high median pressure, with a median pressure of 0.1 to 50.5 MPa, and the mercury unsaturated volume varies significantly, generally between 10% and 20%, corresponding to the JZ3 and KZ2 samples. The Type II pore structure corresponds to a medium porosity and medium permeability reservoir, which is a medium-quality reservoir type in the study area, with a porosity of 15% to 20% and a permeability of $10\times10^{-3}\mu m^2$ to $500\times10^{-3}\mu m^2$. The reservoir rocks corresponding to this pore structure are mainly medium to fine sandstones, with the main storage spaces being residual intergranular pores and intragranular dissolution pores.

Type II pore structures have smaller throat sizes compared to Type I pore structures, with the curve morphology overall slightly leaning towards the upper right, indicating that the connectivity of the reservoir has deteriorated and the permeability has decreased. The throats are mainly concentrated between 7 to 10μm, accounting for more than 50%. The straight section of the curve is relatively short, reflecting that the throats have some degree of sorting, but the sorting is poor. The displacement pressure is low to moderate, ranging from 0.03 to 0.05 MPa, and the median pressure is moderate to high, ranging from 0.1 to 50.5 MPa. The mercury unsaturated volume varies significantly, generally between 10% and 20%, corresponding to the JZ3 and KZ2 samples. Type II pore structures correspond to medium porosity and medium permeability reservoirs, which are the average reservoir types in the study area, with porosities ranging from 15% to 20% and permeabilities ranging from $10\times10^{-3}\mu m^2$ to $500\times10^{-3}\mu m^2$. The reservoir rocks corresponding to this pore structure are mainly medium to fine sandstones, with the main storage spaces being residual intergranular pores and intragranular dissolution pores.

Type III pore structure mercury injection curves lack a straight segment and exhibit a linear state, with the curve

overall leaning towards the upper right, indicating that the pore structure of this type of reservoir is poor, and both the connectivity and permeability of the reservoir are relatively weak. The distribution frequency band of the throats is wide, with almost no peak value, and the distribution frequency in each frequency band is less than 15%, indicating no sorting of the throats, with the development of both micro- and coarse throats, mainly micro-fine throats; the displacement pressure is moderate, with a displacement pressure greater than 0.5 MPa, the median pressure is relatively high, generally greater than 5 MPa, and the mercury unsaturated volume is relatively large, generally greater than 20%, corresponding to the JZ10 sample. The Type III pore structure corresponds to low-ultra-low porosity, low-ultra-low permeability reservoirs, which are the poorer reservoir types in the study area, with porosities less than 15% and permeabilities less than $10\times10^{-3}\mu m^2$. The reservoir rocks corresponding to this pore structure are mainly medium-fine sandstones and fine sandstones, with developed matrix and cementation, and the storage space is mainly poorly developed fine residual intergranular pores and intragranular dissolution pores.

Overall, the reservoirs in the study area are predominantly characterized by Type II pore structures, with Type I pore structures being secondary.

4. Summary

1) The reservoir lithology in the G162 area of the Jiyuan Oilfield in the Ordos Basin is predominantly feldspathic sandstone, with lithic feldspathic sandstone being secondary; the storage space is mainly intergranular pores, with minor development of intragranular dissolution pores; the particle sorting is moderate, and the roundness is primarily sub-angular to sub-rounded; it has a grain-supported framework, with particle-to-particle contact modes dominated by point-line and line contacts; the cementation type is primarily vuggy cementation; and it exhibits characteristics of geo-maturity and medium to high structural maturity.

2) The reservoir in the G162 area of the Jiyuan Oilfield, Yanchang Formation, Section 9, exhibits significant variations in porosity and permeability, with medium-porosity and medium-permeability dominating; there is a good positive correlation between porosity and permeability, indicating an overall better pore structure.

3) The capillary pressure curves of the reservoir in the G162 area of the Jiyuan Oilfield, Yanchang Formation, Section 9, generally exhibit characteristics of low displacement pressure, medium-low median pressure, large median pore throat radius, and medium mercury extraction efficiency. This indicates that the reservoir has a high degree of pore connectivity, good sorting of pore throats, and relatively coarse sizes, suggesting a well-developed pore structure.

4) Based on the types of reservoir pores, physical properties, and the curve morphology and various parameters of high-pressure mercury injection, the reservoirs of the Sha Siya segment in the Luojia area can be classified from good to poor into three types: I, II, and III. The study area is primarily dominated by Type II, followed by Type I.

References

[1] Singh J, Singh U, Garcia R G, et al. Putting the genie back in the bottle: Decarbonizing petroleum with direct air capture and enhanced oil recovery[J]. International Journal of Greenhouse Gas Control, 2024, 139104281-104281.

[2] Zhu X, Qu X, Zhang H, et al. Characteristics and main controlling factors of the Sangonghe tight sandstone reservoirs in the Shengbei Sub-sag of the Turpan-Hami basin, China[J]. Marine and Petroleum Geology, 2025, 171107181-107181.

[3] Gao Y, Lei L, Zhang M, et al. Boosting floating photovoltaics via cooling methods and reservoir characteristics: Crafting optimal symbiosis with off-river pumped hydro storage[J]. Energy, 2024, 312133501-133501.

[4] Wang Y, Bai L, Zhang Y, et al. Reservoir Characteristics and Influencing Factors of Organic-Rich Siliceous Shale of the Upper Permian Dalong Formation in Western Hubei[J]. Energies, 2023, 16(13).

[5] Taotao C, Mo D, Juanyi X, et al. Reservoir characteristics of marine–continental transitional shale and gas-bearing mechanism: Understanding based on comparison with marine shale reservoir[J]. Journal of Natural Gas Geoscience, 2023, 8 (3): 169-185.

[6] Kunpeng X, Yu L, Tao Y, et al. Numerical simulation of gas hydrate production in shenhu area using depressurization: The effect of reservoir permeability heterogeneity[J]. Energy, 2023, 271.

[7] Changwei L, Keyu L, Jianliang L. A petroliferous Ediacaran microbial-dominated carbonate reservoir play in the central Sichuan Basin, China: Characteristics and diagenetic evolution [J]. Precambrian Research, 2023, 384.

[8] M. G M, Yaro P, M. J M, et al. Characterization of volcanic reservoirs; insights from the Badejo and Linguado oil field, Campos Basin, Brazil[J]. Marine and Petroleum Geology, 2022, 146.

[9] Binchi Z, Ma L, Wen G L. Study on characteristics of tight oil reservoir in Ansai Area of Ordos Basin– take the Chang 6 section of Ordos Basin as an example[J]. European Journal of Remote Sensing, 2022, 55(sup1): 3-11.

[10] Xiaozhi W, Qiulin G, Wei Z, et al. Characteristics of Volcanic Reservoirs and Hydrocarbon Accumulation of Carboniferous System in Junggar Basin, China[J]. Journal of Earth Science, 2021, 32(4): 972-985.

[11] Ye Y, Liu S, Ran B, et al. Characteristics of black shale in the Upper Ordovician Wufeng and lower Silurian Longmaxi formations in the Sichuan Basin and its periphery, China[J]. Australian Journal of Earth Sciences, 2017, 64(5): 667-687.

[12] Wu H, Hu W, Cao J, et al. A unique lacustrine mixed dolomitic-clastic sequence for tight oil reservoir within the middle Permian Lucaogou Formation of the Junggar Basin, NW China: Reservoir characteristics and origin[J]. Marine and Petroleum Geology, 2016, 76115-132.